Electronic Supplementary Information

The dependence of oxygen sensitivity on molecular structures of Ir(III) complexes and application for photostable and reversible luminescent oxygen sensing

Yang Xing,[a] Chengfang Qiao,[b] Xinmin Li,[c] Chun Li,[a] Honghao Wang,[a] Fayun Li,[a] Ling Di,*[ad] Zhanxu Yang*[a]

[a] *College of Chemistry, Chemical Engineering, and Environmental Engineering, Liaoning Shihua University, Fushun 113001, China. E-mail: diling@lnpu.edu.cn (L. Di); zxyanglnpu@163.com (Z. Yang)*

[b] *College of Chemical Engineering and Modern Materials, Shangluo University, Shangluo 726000, China*

[c] *School of Pharmacy, Zunyi Medical University, Zunyi, 563000, China.*

[d] *State Key Laboratory of Fine Chemicals, Dalian University of Technology, Linggong Road 2, Dalian 116024, China.*

Contents

2-(3-Bromophenyl)pyridine. ^{1}H NMR (500 MHz, $CDCl_3$): δ 8.70 (d, 1H), 8.17 (s, 1H), 7.91 (d, 1H), 7.77 (td, 1H), 7.71 (d, 1H), 7.54 (dd, 1H), 7.34 (t, 1H), 7.29–7.25 (m, 1H).[1]

Ir(ppy)$_3$: ^{1}H NMR (500 MHz, $CDCl_3$) δ 7.87 (d, 3H), 7.65 (d, 3H), 7.58 (t, 3H), 7.53 (d, 3H), 6.87 (dd, 12H).[2]

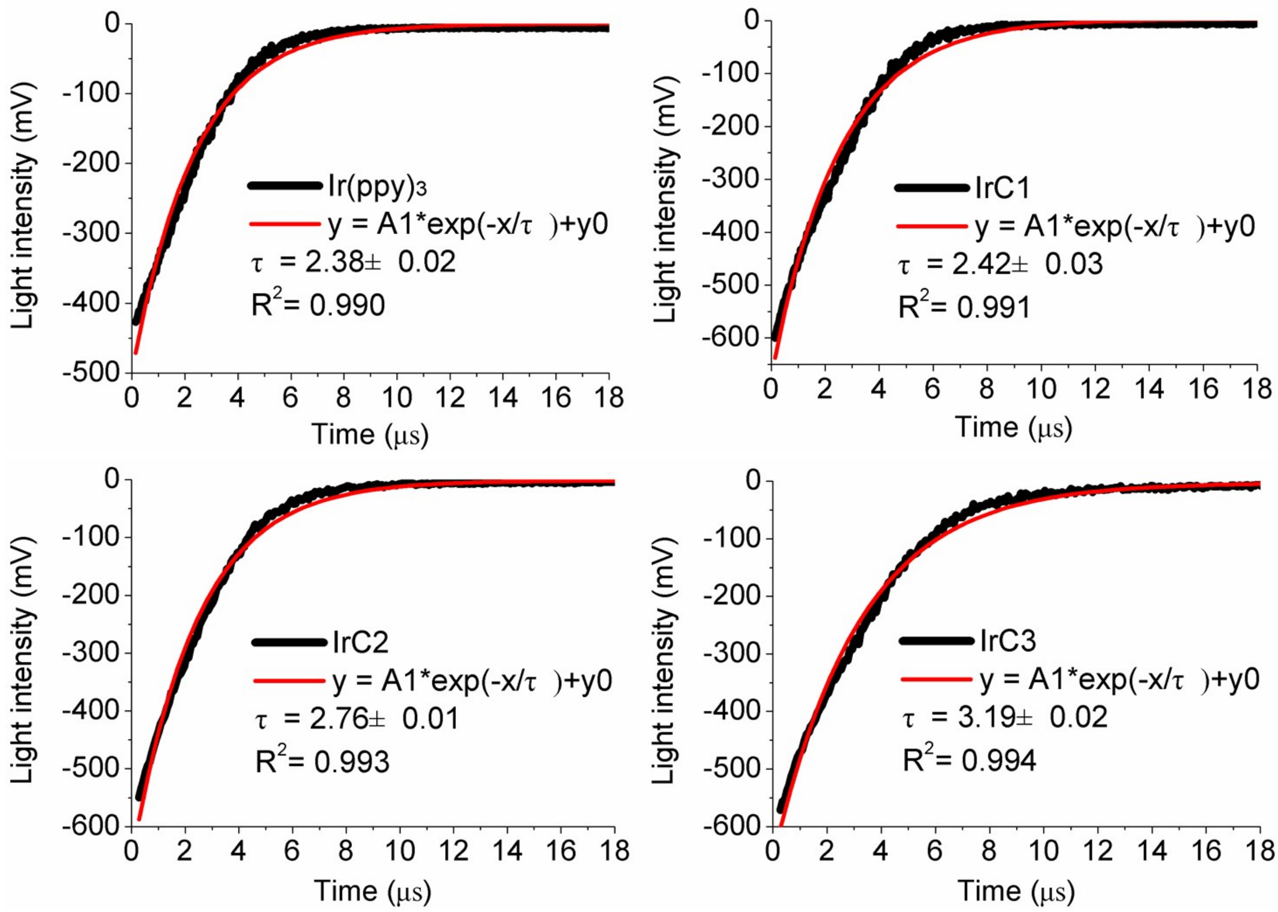

Fig. S1. Luminescent decay curves of Ir(III) complexes in degassed THF. Monoexponential decay regression gave lifetimes.

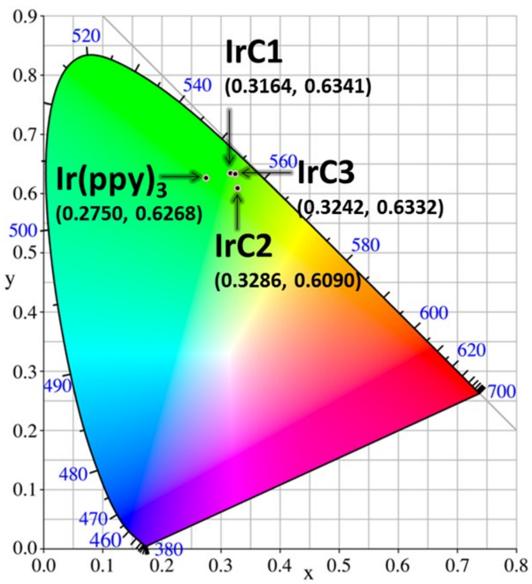

Fig. S2. CIE plots for Ir(III) complexes.

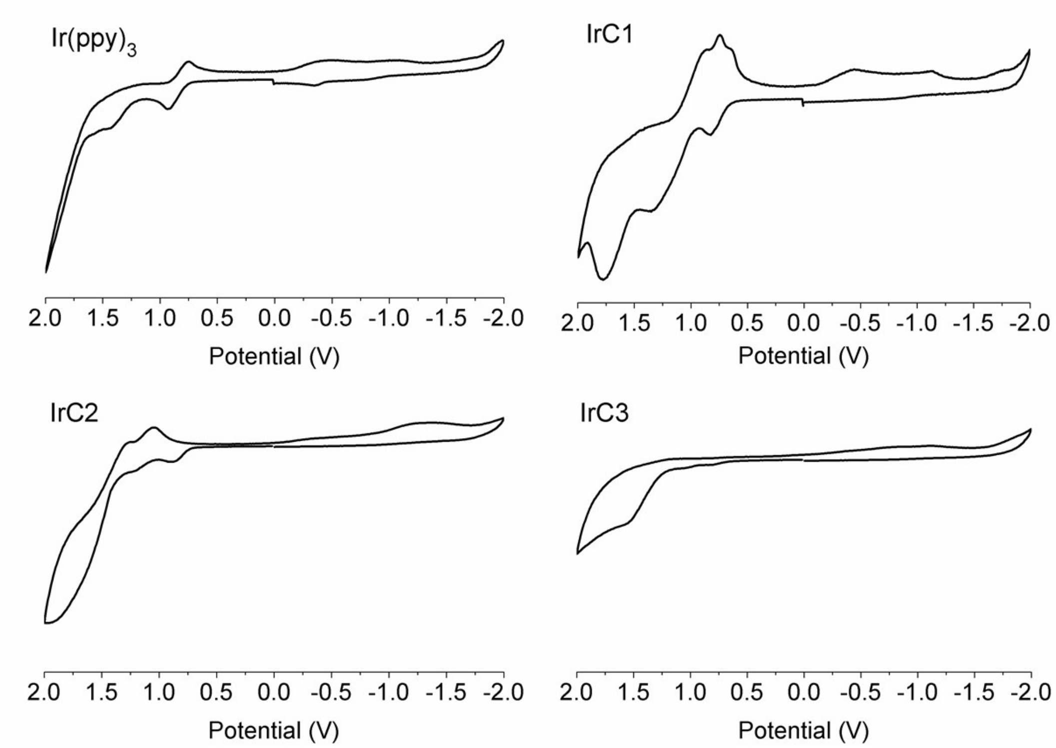

Fig. S3. Cyclic voltammograms of IrC1-IrC3 and $Ir(ppy)_3$. 0.1 M $[Bu_4N]PF_6$ in THF, scan rate 100 mV s^{-1}, measured using saturated calomel electrode (SCE) as the standard.

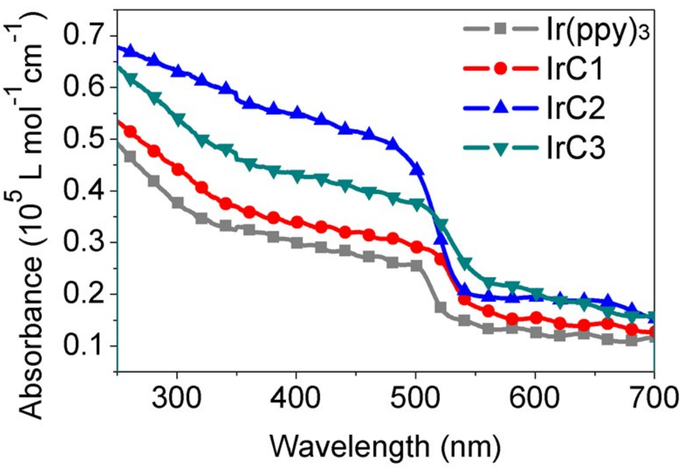

Fig. S4. The solid UV-vis spectra of IrC1-IrC3 and $Ir(ppy)_3$

Table S1. Parameters of oxygen sensing of IrC1-IrC3 and $Ir(ppy)_3$ (fitting of the result to the two-site model).

Complexes	λ_{ex}(nm)	λ_{em}(nm)	f_1 [a]	f_2 [a]	K_{SV1} [b]	K_{SV2} [b]	r^2 [c]	K_{SV}^{app} [d]
$Ir(ppy)_3$	400	511	0.985	0.015	121.4	0.00001	0.99983	119.6
IrC1	400	522	0.998	0.002	202.6	0.00001	0.99985	202.2
IrC2	400	516	0.999	0.001	144.2	0.00001	0.99948	144.1
IrC3	400	525	0.999	0.001	181.3	0.00001	0.99978	181.1

[a] Ratio of the two portions of the Ir(III) complexes. [b] Quenching constant of the two portions(bar^{-1}). [c] Determination coefficients. [d] Weighted quenching constant (bar^{-1}).

Table S2. The phosphorescent decay times (τ), emission intensity ratios (I_0/I_{100}-1), and the ratios of collision radii ($\sigma_{Ir(III)}/\sigma_{Ir(ppy)3}$) of all the Ir(III) complexes.

Ir(III) complexes	Data	1	2	3	4	5	Mean	Standard
$Ir(ppy)_3$	I_0	511.3	518.6	511.6	532.6	536.4	522.10	11.77
τ_0 (2.38 μs)	I_{100}	6.4	5.9	6.3	6.3	6.0	6.18	0.22
	I_0/I_{100}-1	78.4	86.9	80.6	83.4	88.1	83.48	4.10
IrC1	I_0	871.1	930.1	900.1	857.4	857.6	883.26	31.43
τ_0 (2.42 μs)	I_{100}	5.1	4.7	4.9	4.9	4.7	4.86	0.17
	I_0/I_{100}-1	169.8	194.4	181.9	174.7	181.8	180.52	9.29
	$\sigma_{IrC1}/\sigma_{Ir(ppy)3}$	2.13	2.20	2.22	2.06	2.03	***2.13***	0.08
IrC2	I_0	989.6	936.5	941.7	967.1	956.4	958.26	21.28
τ_0 (2.76 μs)	I_{100}	8.6	7.0	7.9	8.6	7.6	7.94	0.68
	I_0/I_{100}-1	114.1	133.0	116.8	111.2	124.6	119.94	8.84
	$\sigma_{IrC2}/\sigma_{Ir(ppy)3}$	1.25	1.32	1.25	1.15	1.22	***1.24***	0.06
IrC3	I_0	411.3	426.8	438.1	415.5	420.7	422.48	10.48
τ_0 (3.19 μs)	I_{100}	2.6	2.5	2.5	2.2	2.4	2.44	0.15
	I_0/I_{100}-1	157.2	172.3	171.8	185.5	173.6	172.08	10.05
	$\sigma_{IrC3}/\sigma_{Ir(ppy)3}$	1.50	1.48	1.59	1.66	1.47	***1.54***	0.08

Table S3. Data of spin population analysis of IrC1-IrC3 and $Ir(ppy)_3$.

	Type	P_α [a]	P_β [b]	$P_{\alpha+\beta}$ [c]	P_{spin} [d]	$P_{spin\%}$ [e]
$Ir(ppy)_3$	*s* orbitals	69.46972	69.40729	138.87701	0.06243	3.12%
	p orbitals	56.91048	55.35288	112.26335	1.55760	77.88%
	d orbitals	4.61980	4.23983	8.85964	0.37997	19.00%
IrC1	*s* orbitals	177.16242	177.08660	354.24902	0.07581	3.80%
	p orbitals	140.12143	138.45833	278.57975	1.66310	83.15%
	d orbitals	5.71616	5.45507	11.17123	0.26109	13.05%
	TPA moieties	193.54344	193.31140	386.85484	**0.23210**	**11.61%**
IrC2	*s* orbitals	174.46512	174.38946	348.85457	0.07566	3.78%
	p orbitals	139.77163	138.17281	277.94444	1.59881	79.94%
	d orbitals	5.76326	5.43773	11.20098	0.32553	16.28%
	Cz1 moieties	190.55660	190.46800	381.02460	**0.08862**	**4.43%**
IrC3	*s* orbitals	174.49119	174.41387	348.90506	0.07732	3.87%
	p orbitals	139.75181	138.13165	277.88347	1.62016	81.00%
	d orbitals	5.75700	5.45448	11.21148	0.30252	15.13%
	Cz2 moieties	190.51510	190.38310	380.89820	**0.13201**	**6.60%**

[a] Population of α electron. [b] Population of β electron. [c] Population of α and β electron, $P_{\alpha+\beta}=P_\alpha+P_\beta$. [d] Spin population, $P_{spin}=P_\alpha-P_\beta$. [e] Percentages of spin population, $P_{spin\%}=(100P_{spin}/2.00000)\%$.

The limits of detection (LODs) of IrC1-IrC3 and Ir(ppy)$_3$ in THF [3]

Limit of detection (LOD) $$LOD = \frac{(S/N) \times 10^{-3}}{K_{SV}^{app}}$$

Signal to noise ratio (S/N) $$S/N = 20\log\left(U_1/U_0\right)$$ U_1: Signal amplitude U_0: Noise amplitude

Ir(ppy)$_3$: U_1 = 511.3, U_0 = 1.3, S/N =51.9, LOD = 0.43 mbar

IrC1: U_1 = 871.1, U_0 = 1.3, S/N = 56.5, LOD = 0.27 mbar

IrC2: U_1 = 989.6, U_0 = 1.3, S/N = 57.6, LOD = 0.40 mbar

IrC3: U_1 = 411.3, U_0 = 1.3, S/N = 50.0, LOD = 0.28 mbar

Table S4. Parameters of oxygen sensing films of IrC1-IrC3 and Ir(ppy)$_3$ with EC as the supporting matrix (fitting of the result to the two-site model).

Complexes	λ_{ex}(nm)	λ_{em}(nm)	f_1[a]	f_2[a]	K_{SV1}[b]	K_{SV2}[b]	r^2[c]	K_{SV}^{app}[d]
Ir(ppy)$_3$	400	511	0.997	0.003	8.9	0.00001	0.99828	8.8
IrC1	400	522	0.999	0.001	33.0	0.00001	0.99789	32.9
IrC2	400	516	0.911	0.089	20.3	0.00001	0.96328	18.5
IrC3	400	525	0.978	0.022	24.1	0.00001	0.99578	23.6

[a] Ratio of the two portions of the Ir(III) complexes. [b] Quenching constant of the two portions(bar^{-1}). [c] Determination coefficients. [d] Weighted quenching constant (bar^{-1}).

References.

1 Y. Xing, C. Liu, J.-H. Xiu and J.-Y. Li, *Inorg. Chem.*, 2015, **54**, 7783.

2 A. B. Tamayo, B. D. Alleyne, P. I. Djurovich, S. Lamansky, I. Tsyba, N. N. Ho, R. Bau and M. E. Thompson, *J. Am. Chem. Soc.*, 2003, **125**, 7377.

3 X. D. Wang and O. S. Wolfbeis, *Chem. Soc. Rev.*, 2014, **43**, 3666.